Electrostatic modulation of anisotropic magnetotransport in Ar+-irradiated SrTiO3: Effects of boundary scattering

J. H. Ngai,[1] Y. Segal,[1] F. J. Walker,[1] and C. H. Ahn[1,2]

[1]*Department of Applied Physics, and Center for Research on Interface Structures and Phenomena, Yale University, 15 Prospect Street, New Haven, Connecticut 06520-8284, USA*

[2]*Department of Physics, Yale University, 217 Prospect Street, New Haven, Connecticut 06511-8499, USA*

We present low temperature, magnetotransport measurements on a quasi-two-dimensional electron gas created by Ar+-irradiation of SrTiO3. We observe negative (positive) magnetoresistance for fields applied in (out of) the plane of the electron gas. By modulating the mobility μ of the electron gas through an electrostatic field, we find the in-plane magnetoresistance is a function of the cyclotron frequency. The negative in-plane magnetoresistance can be explained by a drop in boundary scattering, which occurs as the cyclotron orbits become smaller than the finite thickness of the electron gas. These results elucidate the critical role boundary scattering plays in the magnetotransport of quasi-two-dimensional electron gases. The implications of these results on recent magnetotransport measurements of LaAlO3/SrTiO3 samples are discussed.

I. INTRODUCTION

Quasi-two-dimensional electron gases (Q2DEG), formed by modulating the charge carrier density near interfaces and surfaces of SrTiO3 (STO),[1] exhibit rich phenomena that can potentially extend the functionality of transition metal oxides. In particular, much interest has focused on the Q2DEG found at the interface between LaAlO3 (LAO) and STO.[2] Several doping mechanisms have been proposed to explain the origin of the Q2DEG, including a polar discontinuity in the LAO,[3] oxygen vacancies in the STO,[4] and cation mixing of Sr and La at the interface.[5] The latter mechanism has gained increased attention in light of recent experiments.[6,7] Beyond the doping mechanism, an issue of key importance is determining whether the Q2DEG at the LAO/STO interface exhibits behavior that cannot be explained by the properties of doped STO.

In this regard, evidence for magnetic behavior at the LAO/STO interface is particularly intriguing[8–11] since LAO and STO are both nonmagnetic. Thus far, the evidence for magnetism has been based largely on the observation of negative magnetoresistance (MR), which can be associated with the suppression of spin disorder. Negative MR has been measured in LAO/STO samples exhibiting both high and low sheet resistances R_s.[9–11] For the high R_s samples, negative MR exhibiting hysteresis has been observed for fields applied both in and out of the plane of the Q2DEG. For low R_s samples, the MR is highly anisotropic. Negative (positive) MR is observed for fields applied in (out of) the plane of the Q2DEG.[10,11]

It is essential to determine whether the negative in-plane MR is unique to the LAO/STO interface, or if this effect can, in general, be observed in STO that has been doped near an interface or surface. The former scenario would suggest the particular electronic structure of the LAO/STO interface gives rise to negative in-plane MR, while the latter would point to a geometric origin. A study of the magnetotransport of Ar+ irradiation of STO could shed light on this issue. Ar+ irradiation creates a thin layer of oxygen vacancies near the surface, a doping mechanism that is now well understood.[12–15]

Furthermore, oxygen deficient STO is not known to be magnetic. With striking similarity to low R_s LAO/STO samples, we observe negative (positive) MR for fields B ($= \mu_0 H$) applied in (out of) the plane of the Q2DEG. By modulating the mobility μ of the Q2DEG through an electrostatic field, we find the in-plane MR is a function of $\mu B = \omega_c \tau$, which indicates the presence of cyclotron orbits confined within the finite thickness of the Q2DEG, where ω_c and τ are the cyclotron frequency and carrier relaxation time, respectively. The negative in-plane MR can be explained by a drop in boundary scattering, which occurs as the cyclotron orbits of carriers become smaller than the finite thickness of the Q2DEG. Our results elucidate the critical role boundary scattering plays in the magnetotransport properties of Q2DEG's, and provide a nonmagnetic explanation for the negative MR observed in low R_s LAO/STO samples.

II. EXPERIMENTAL PROCEDURE

A schematic of our Ar+-irradiated devices is shown in Fig. 1(a). An 80×40 μm Hall bar is defined using standard photolithography on a 0.5-mm thick STO substrate. The device becomes conducting after irradiation with 1.1 keV Ar+ ions at a rate of $\sim 3.7 \times 10^{12}$ cm^{-2}s^{-1} for 90 minutes in an ultrahigh vacuum chamber. It was shown in a previous study[15] that irradiation under these conditions creates a $\sim$5-nm thick oxygen-deficient crystalline layer, which is situated between an amorphous top layer and the undoped substrate below. The amorphous top layer is insulating, with the conduction occurring in the crystalline STO, where the thin layer of oxygen vacancies act as dopants that create the Q2DEG. Ohmic contacts are formed by wire bonding Al wires directly to the STO, while the gate contact is made by depositing Au on the back side of the device. All measurements are performed at $T = 2$ K to minimize inelastic scattering from phonons.

We note that the $\sim$5-nm depth of oxygen vacancies we observed[15] is roughly an order of magnitude smaller than the depth reported by Herranz *et al.*[16] Surprisingly, the much larger
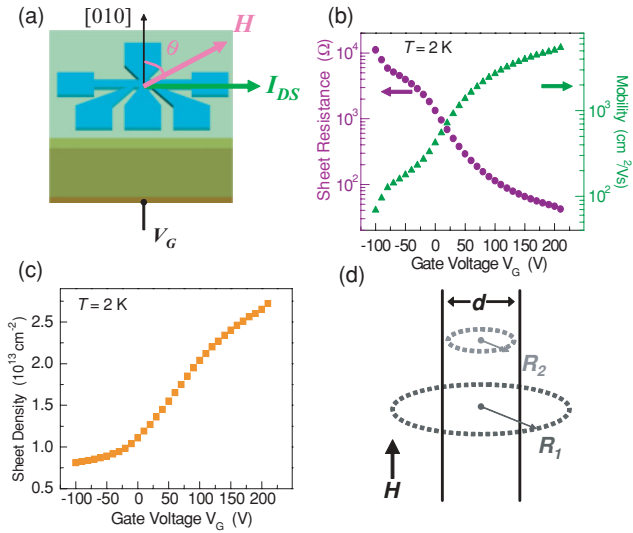
FIG. 1. (Color online) Characterization of Ar$^+$-irradiated STO devices at $T = 2$ K. (a) Schematic illustrating the device and the direction of the in-plane field H. H is applied at an angle θ relative to the current I_{DS}, which is applied along the [100] crystallographic direction. (b) Sheet resistance (mobility) versus V_G shown as circles (triangles). (c) Sheet carrier density versus V_G. (d) Cross-sectional illustration of a thin conducting plate of thickness d. Orbital radius $R_1 > (d/2)$ [$R_2 < (d/2)$].

vacancy depth measured by Herranz *et al.* was achieved by irradiating with less energetic ions $\sim$300 eV. However, we note that the total areal density of ions irradiated over time was two orders of magnitude larger in their study, suggesting this latter quantity also affects the depth of vacancies created.

III. RESULTS AND DISCUSSION

Figure 1(b) (circles) indicates that R_s can be modulated by over two orders of magnitude with gate voltage V_G. For positive (negative) V_G, R_s decreases (increases), consistent with the addition (removal) of *n*-type carriers to (from) the channel of the device according to the relation $R_s = (n_s e \mu)^{-1}$, where e is the electron charge and n_s is the sheet carrier density. Hall measurements at each V_G directly determined Δn_s. We find that n_s can be tuned from $\sim$8 to $\sim$27 $\times 10^{12}$ cm^{-2} as shown in Fig. 1(c). This modest change in n_s does not account for ΔR_s, thus the principal effect of V_G is the modulation of μ, as shown in Fig. 1(b) (triangles). For the device shown, μ can be modulated by a factor of $\sim$80, from $\sim$70 to $\sim$5500 cm^2/Vs.

Our Ar$^+$-irradiated devices exhibit highly anisotropic MR that can be modulated through V_G. The MR, defined as $\Delta R_s(H)/R_s(0)$, where $\Delta R_s(H) = R_s(H) - R_s(0)$, is shown for fields applied out of the plane of the device in Fig. 2(a). Positive MR is observed, with the magnitude increasing for higher V_G. In contrast, negative MR is observed for fields applied in the plane of the Q2DEG, with the magnitude increasing for higher V_G as shown in Figs. 2(b) and 2(c). The in-plane MR is measured using the experimental geometry shown in Fig. 1(a). R_s is measured as the angle θ of the applied field is varied with respect to the [010] direction of the crystal.

The probe current I_{DS} is fixed along the [100] direction of the crystal.

The in-plane MR is a function of both μ and B. For fixed V_G (i.e., fixed μ) the in-plane MR can be modulated with B, as shown by the data points in Fig. 2(b). The solid lines, which are fits to the data, will be discussed shortly. A qualitatively similar evolution of the in-plane MR can be achieved by modulating μ for fixed B, as shown in Fig. 2(c). The complementary dependence on μ and B suggests the in-plane MR is a function of $\mu B = \omega_c \tau$.

To establish the dependence of the MR on $\omega_c \tau$, we fit our data using a generalized resistivity tensor

$$\rho_{ij}(\alpha) = \sum_{k,l,m,\dots,=1}^{3} (c_{ij} + c_{kij}\alpha_k + c_{klij}\alpha_k\alpha_l$$
$$+ c_{klmij}\alpha_k\alpha_l\alpha_m + c_{klmnij}\alpha_k\alpha_l\alpha_m\alpha_n + \cdots). \quad (1)$$

Here, the c's and α's are, respectively, the polynomial expansion coefficients and direction cosines of the magnetic field with respect to I_{DS}. Typically an expansion of the tensor to second order (i.e., a quadratic approximation) is often sufficient to describe the MR in semiconductors for $\omega_c \tau < 1$.[17] The highly nontrivial MR shown in Fig. 2 indicates higher-order terms are necessary to describe our data. For our devices, B is applied within the plane of a cubic crystal and I_{DS} is fixed along the [100]. The tensor can then be simplified to

$$\frac{\Delta R_s(B)}{R_s(0)} = C_0 + C_2\cos(2\theta) + C_4\cos(4\theta) + C_6\cos(6\theta),$$
(2)

where coefficients C_0, C_2, C_4, and C_6 represent the zeroth, second, fourth, and sixth order contributions to the MR, respectively. Representative fits using Eq. (2) are shown as solid lines in Figs. 2(b) and 2(c).

The dependence of the MR coefficients on $\omega_c \tau$ indicates the in-plane MR arises from orbital motion. For $\mu B < 1$, the coefficients C_0, C_2, C_4, and C_6 scale to a common curve for each V_G, as shown in Figs. 3(a), 3(b), 3(c), and 3(d), respectively. This scaling behavior indicates Kohler's rule is obeyed (i.e., the in-plane MR is a function of $\omega_c \tau$[18]). Thus, carriers follow curved trajectories of radii $R \propto B^{-1}$, induced by the Lorentz force of the in-plane field. The presence of these cyclotron orbits for in-plane fields indicates carrier dispersion along k_z, the direction normal to the Q2DEG plane.

The MR in our devices bears striking similarities to the MR observed in low R_s LAO/STO samples, namely negative (positive) behavior for in-plane (out of plane) fields[10,11] and an anisotropic dependence on the direction of the in-plane field with respect to the probe current.[10] Shalom *et al.* attributed the negative in-plane MR in their LAO/STO samples to a magnetic origin.[10] Applying a similar analysis to our Ar$^+$-irradiated Q2DEG's would suggest that oxygen vacancies alone can give rise to magnetic behavior. While evidence for magnetism induced by oxygen vacancies has been found in various semiconducting oxides,[19] oxygen-deficient STO has not been found to be magnetic.

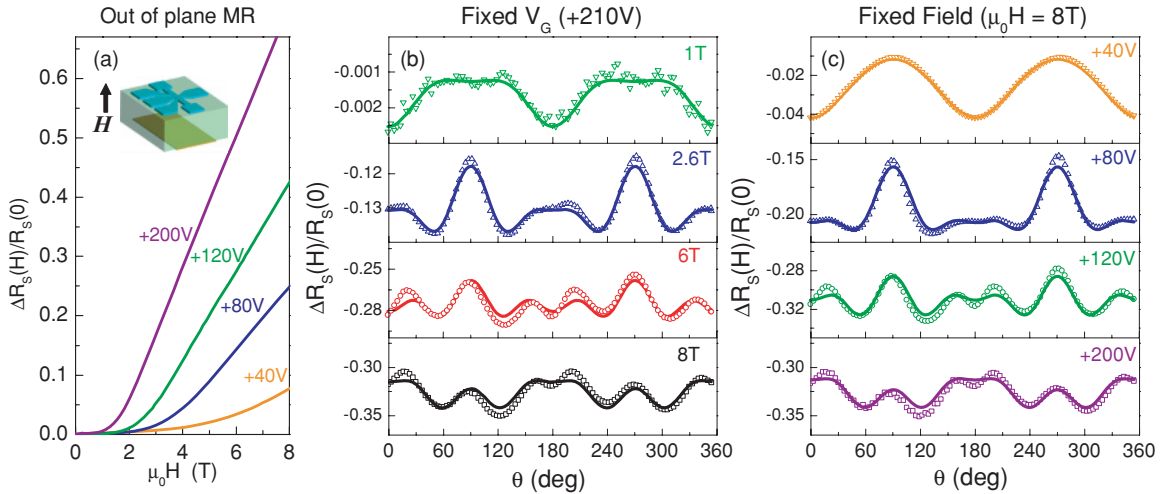Instead, we propose an alternative explanation based on a reduction of diffusive boundary scattering. Boundary

FIG. 2. (Color online) Electric field control of magnetoresistance in Ar$^+$-irradiated STO at $T = 2$ K. (a) MR for fields applied out of the plane of the Q2DEG for various V_G. Note the sign of the MR is positive. (b) Modulation of in-plane MR with B for fixed $V_G = +210$ V. Note the sign of the MR is negative. Experimental data are shown as points, with the fits (solid lines) obtained using Eq. (2). (c) Modulation of in-plane MR with V_G for fixed $B = 8$ T. Note the similar dependence of the in-plane MR on V_G and B.

scattering arises as the thickness d of the Q2DEG becomes comparable to the mean free path l in the bulk. A reduction in boundary scattering occurs as orbital radii R become $\leqslant d/2$ in increasing fields, as heuristically illustrated in Fig. 1(d). A reduction in diffusive or nonspecular boundary scattering results in negative MR.[20] Such behavior has been observed and studied in thin metallic films.[20–23]

The in-plane MR coefficients exhibit characteristics that are consistent with a loss of diffusive boundary scattering. First, we note that the enhancement of μ with V_G arises from an increase in d of the electron gas.[15] This change in d is captured by the dependence of C_0 on V_G, as shown in Fig. 3(a). For $V_G = +200$ V ($+40$ V), the maximum field of 8 T is (is not) sufficient to induce cyclotron orbits

that have nominal diameters less than d of the Q2DEG, and thus the magnitude of negative MR is large (small). Second, the emergence of negative MR for μB ($\omega_c \tau$) > 1 is consistent with $d \sim l$, the condition denoting significant boundary scattering. For $\omega_c \tau > 1$, the cyclotron period $\tau_c = 1/\omega_c$ becomes less than τ, and thus carriers can execute cyclotron orbits without encountering a scattering event. In terms of length scales, cyclotron diameters become less than l, or in the case of boundary scattering, d. Third, a positive inflection in C_0 emerges at higher μB, suggesting saturation. Saturation is also expected since a further drop in the MR should not occur once diffusive boundary scattering has been eliminated.

To check for self-consistency in our analysis of the negative MR, we follow a method described previously[15] to calculate l, d, and the Fermi wavelength λ_F, as summarized in Table I. The condition for boundary scattering $d \sim l$ holds for all V_G. The largely constant λ_F can be attributed to the concomitant increase in n_s, which offsets the enhancement in d with V_G. As V_G increases, the electron gas becomes more three-dimensional as d far exceeds λ_F.

A complete quantitative analysis of the MR coefficients is beyond the scope of this work. For bulk crystals, the quantitative values of MR coefficients depends greatly on the Fermi surface topology and the k dependence of scattering mechanisms.[18,24] For our devices, a quantitative analysis of the MR coefficients is further complicated by boundary scattering
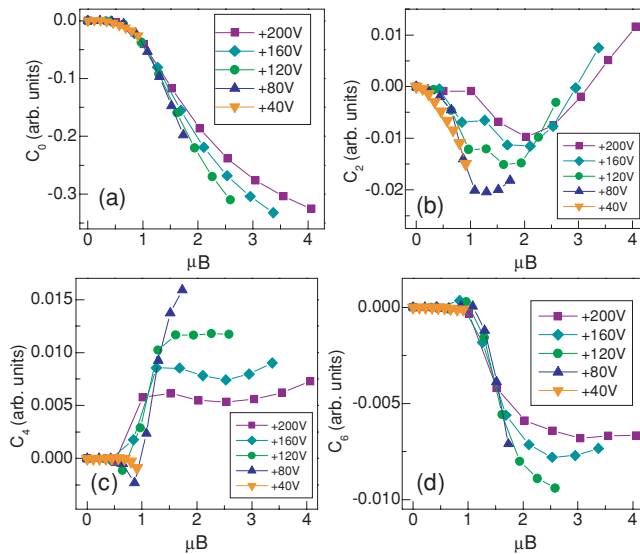

FIG. 3. (Color online) Evolution of the in-plane magnetoresistance tensor coefficients with μB for various V_G. (a) C_0, (b) C_2, (c) C_4, and (d) C_6.

TABLE I. Q2DEG mean-free path and thickness.

V_G (V)	l (nm)	d (nm)	λ_F (nm)
+40	28	86	17
+80	57	87	16
+120	80	124	17
+160	102	150	17
+200	119	174	18

and the electrostatic confinement of the electron gas. The latter modifies the k-space topology in the direction of confinement, leading to quantized subbands in the two-dimensional limit. We note for $\mu B > 1$, nonscaling of the MR coefficients emerges, indicating the change in scattering induced by V_G cannot be captured by scaling τ by a factor λ (i.e., $\tau \to \lambda\tau$[18] where $\tau^{-1} = \tau_{\text{bulk}}^{-1} + \tau_{\text{boundary}}^{-1}$). A loss in boundary scattering is consistent with nonscaling since $\tau_{\text{boundary}}^{-1} \to \infty$.

Finally, we discuss the effect temperature has on the confinement or thickness of a Q2DEG. The emergence of negative in-plane MR below 35 K in low R_s LAO/STO samples was interpreted to indicate the onset of antiferromagnetic behavior.[10] We have demonstrated that the appearance of negative in-plane MR arises from an increase in the thickness of the Q2DEG.[15] Here we argue the temperature dependence of the negative MR in LAO/STO samples can also be attributed to an increase in thickness. Due to proximity to a ferroelectric instability, the dielectric constant ϵ of STO diverges at low temperatures, reaching as high as $\sim$24,000ϵ_0.[25] The increase in ϵ can give rise to a decrease in the confinement of carriers near the interface, particularly for LAO/STO samples that have sheet carrier densities less than 6×10^{13} cm^{-2} (Refs. 4,26) On the premise the negative MR measured in low R_s LAO/STO samples arises from a loss in boundary scattering[10] analysis using our methodology[15] indicates the Q2DEG thickness in these samples is $\geqslant$50 nm.

IV. SUMMARY

In summary, we have performed low temperature, magnetotransport measurements of Ar$^+$-irradiated STO field-effect devices. Similar to low R_s LAO/STO samples, negative (positive) MR is observed for fields applied in (out of) the plane of our devices. The negative in-plane MR varies anisotropically with the direction of the in-plane field with respect to the applied current. By modulating the μ of the Q2DEG through an electrostatic field, we find the in-plane MR is a function of $\omega_c \tau$, indicating the presence of orbital motion confined within the finite thickness of the Q2DEG. We find the negative in-plane MR can be explained by a drop in diffusive boundary scattering, which occurs as cyclotron orbits become smaller than the finite thickness of the Q2DEG. These findings point to the critical role boundary scattering plays in the magnetotransport properties of Q2DEG's. Furthermore, our results provide a nonmagnetic explanation for the negative MR observed in low R_s LAO/STO samples.

[1] O. N. Tufte and P. W. Chapman, Phys. Rev. **155**, 796 (1967).

[2] A. Ohtomo and H. Y. Hwang, Nature (London) **427**, 423 (2004).

[3] S. Thiel, G. Hammerl, A. Schmehl, C. W. Schneider, and J. Mannhart, Science **313**, 1942 (2006).

[4] W. Siemons, G. Koster, H. Yamamoto, W. A. Harrison, G. Lucovsky, T. H. Geballe, D. H. A. Blank, and M. R. Beasley, Phys. Rev. Lett. **98**, 196802 (2007).

[5] P. R. Willmott, S. A. Pauli, R. Herger, C. M. Schlepütz, D. Martoccia, B. D. Patterson, B. Delley, R. Clarke, D. Kumah, C. Cionca, and Y. Yacoby, Phys. Rev. Lett. **99**, 155502 (2007).

[6] A. S. Kalabukhov, Yu. A. Boikov, I. T. Serenkov, V. I. Sakharov, V. N. Popok, R. Gunnarsson, J. Börjesson, N. Ljustina, E. Olsson, D. Winkler, and T. Claeson, Phys. Rev. Lett. **103**, 146101 (2009).

[7] Y. Segal, J. H. Ngai, J. W. Reiner, F. J. Walker, and C. H. Ahn, Phys. Rev. B **80**, 241107(R) (2009).

[8] R. Pentcheva and W. E. Pickett, Phys. Rev. B **74**, 035112 (2006).

[9] A. Brinkman, M. Huijben, M. van Zalk, J. Huijben, U. Zeitler, J. C. Maan, W. G. van der Wiel, G. Rijnders, D. H. A. Blank, and H. Hilgenkamp, Nat. Mater. **6**, 493 (2007).

[10] M. Ben Shalom, C. W. Tai, Y. Lereah, M. Sachs, E. Levy, D. Rakhmilevitch, A. Palevski, and Y. Dagan, Phys. Rev. B **80**, 140403(R) (2009).

[11] S. Seri and L. Klein, Phys. Rev. B **80**, 180410(R) (2009).

[12] V. E. Henrich, G. Dresselhaus, and H. J. Zeiger, Phys. Rev. B **17**, 4908 (1978).

[13] D. W. Reagor and V. Y. Butko, Nat. Mater. **4**, 593 (2005).

[14] V. Y. Butko, H. Wang, and D. Reagor, Nanotechnology **19**, 305401 (2008).

[15] J. H. Ngai, Y. Segal, D. Su, Y. Zhu, F. J. Walker, S. Ismail-Beigi, K. Le Hur, C. H. Ahn, Phys. Rev. B **81**, 241307(R) (2010).

[16] G. Herranz, O. Copie, A. Gentils, E. Tafra, M. Basletic, F. Fortuna, K. Bouzehouane, S. Fusil, E. Jacquet, C. Carretero, M. Bibes, A. Hamzic, and A. Barthelemy, J. Appl. Phys. **107**, 103704 (2010).

[17] G. L. Pearson and H. Suhl, Phys. Rev. **83**, 768 (1951).

[18] R. G. Chambers, Proc. R. Soc. A **238**, 344 (1956).

[19] N. Hong, J. Sakai, and F. Gervais, J. of Mag. and Mag. Mat. **316**, 214 (2007).

[20] Y. S. Way and Y. H. Kao, Phys. Rev. B **5**, 2039 (1971).

[21] D. K. C. MacDonald, Nature (London) **163**, 637 (1949).

[22] M. C. Steele, Phys. Rev. **97**, 1720 (1955).

[23] A. N. Friedman and S. H. Koenig, IBM J. Res. Dev. **4**, 158 (1960).

[24] F. Kuchar and P. Frankus, Phys. Rev. B **16**, 874 (1977).

[25] H.-M. Christen, J. Mannhart, E. J. Williams, and C. Gerber, Phys. Rev. B **49**, 12095 (1994).

[26] O. Copie, V. Garcia, C. Bödefeld, C. Carretero, M. Bibes, G. Herranz, E. Jacquet, J.-L. Maurice, B. Vinter, S. Fusil, K. Bouzehouane, H. Jaffres, and A. Barthelemy, Phys. Rev. Lett. **102**, 216804 (2009).